Available online at www.sciencedirect.com
SCIENCE DIRECT®
Thermochimica Acta 435 (2005) 202–208
thermochimica acta
www.elsevier.com/locate/tca

Methyl methacrylate oligomerically-modified clay and its poly(methyl methacrylate) nanocomposites

Xiaoxia Zheng, David D. Jiang, Charles A. Wilkie *

Department of Chemistry, Marquette University, P.O. Box 1881, Milwaukee, WI 53233, USA

Received 26 March 2005; received in revised form 3 June 2005; accepted 6 June 2005
Available online 12 July 2005

Abstract

A methyl methacrylate oligomerically-modified clay was used to prepare poly(methyl methacrylate) clay nanocomposites by melt blending and the effect of the clay loading level on the modified clay and corresponding nanocomposite was studied. These nanocomposites were characterized by X-ray diffraction, transmission electron microscopy, thermogravimetric analysis and cone calorimetry. The results show a mixed intercalated/delaminated morphology with good nanodispersion. The compatibility between the methylacrylate-subsituted clay and poly(methyl methacrylate) (PMMA) are greatly improved compared to other oligomerically-modified clays.

Keywords: Oligomerically-modified clay; Nanocomposites; Poly(methyl methacrylate); Thermogravimetric analysis; Cone calorimetry

1. Introduction

Research in polymer clay nanocomposites is motivated by the significant improvement in the physical and mechanical properties of the polymer at very low clay loading [1,2]. The common clays are naturally occurring minerals and are typically highly hydrophilic and therefore naturally incompatible with the wide range of hydrophobic polymers. The usual treatment is to ion-exchange the clay cation for an alkylammonium or phosphonium cation, which can contain various substituents, at least one of which must be a carbon chain of 12 carbons or more to change the clay polarity and make the clay organophilic [3]. The preparation of a nanocomposite may be accomplished either by in situ polymerization or by blending, with melt blending the industrially preferred process.

Depending on the interaction between the clay and the polymer, three distinct types of nanocomposites may be produced: immiscible, intercalated and delaminated nanocomposites. An immiscible system contains the clay acting essentially as a filler and it is not nanodispersed; this is also commonly referred to as a microcomposite. Both the intercalated systems and the delaminated systems show nanodispersion, which means that the clay is present at the nanometer level. In an intercalated system the registry between the layers is maintained while this registry is lost in a delaminated system. The design of the modified clay is an essential feature in the type of nanodispersion which may be obtained. Previous work from this laboratory has shown that the presence of one or two styryl group on the cation of the modified clay can produce a completely delaminated polystyrene nanocomposite while two styryl group on the modified clay are required to produce a delaminated poly(methyl methacrylate) nanocomposite [4,5]. A similar conclusion can be reached with one or two methyacrylate units on the cation of the modified clay: one or two methyacrylate group on the modified clay produces a completely delaminated polystyrene nanocomposite while two methyacrylate group are required to produce a delaminated poly(methyl methacrylate) nanocomposite [6]. Zeng and Lee [7] used a monomethacrylate hexdecylammonium bromide modified clay to get a completely delaminated polystyrene nanocomposite and a mixed delaminated/intercalated poly(methyl methacrylate) nanocomposite by in situ polymerization while Huang and Brittain [8] used a monomethacrylate

* Corresponding author. Tel.: +1 414 288 7239; fax: +1 414 288 7066.
E-mail address: charles.wilkie@marquette.edu (C.A. Wilkie).

0040-6031/$ – see front matter © 2005 Elsevier B.V. All rights reserved.
doi:10.1016/j.tca.2005.06.006

trimethylammonium chloride as emulsifier to obtain a delaminated poly(methyl methacrylate) nanocomposite with the pristine sodium clay by emulsion polymerization.

Poly(methyl methacrylate) clay nanocomposites have a potential advantage in reduced flammability, reduced gas permeability and improved thermal and mechanical properties without any loss of optical clarity. In this study, we use a methacrylate oligomerically-modified clay to prepare poly(methyl methacrylate) nanocomposites by melt blending. The effect of clay loading level on the modified clay and its corresponding nanocomposite was studied.

2. Experimental

2.1. Materials

Most of the materials used in this study, including methyl methacrylate, benzoyl peroxide (BPO), inhibitor removal reagent, poly(methyl methacrylate), (inherent viscosity 1.250, $M_w = 996{,}000$, $T_g = 125\,^{\circ}C$), were acquired from the Aldrich Chemical Co. The sample of 2-(dimethyamino)ethylmethacrylate was acquired from TCI, America while 1-bromohexadecane was purchased from Lancaster Chemical Company. The pristine sodium clay was kindly provided by Southern Clay Products Inc.

2.2. Instrumentation

Thermogravimetric analysis (TGA) was performed on SDT 2960 simultaneous TGA-DTA instrument under a flowing nitrogen atmosphere at a scan rate of 10 °C/min from 20 to 600 °C; temperatures are reproducible to ±3 °C, while the error bars on the fraction of nonvolatile material is ±3%. Cone calorimetry was performed using an Atlas Cone 2 instrument according ASTM E 1354 at an incident flux of 35 or 50 kW/m^2 using a cone shaped heater. Exhaust flow was set at 24 L/s and the spark was continuous until the sample ignited. Cone samples were prepared by compression molding the sample (20–50 g) into square plaques using a heated press. Typical results from Cone calorimetry are reproducible to within about ±10%. These uncertainties are based on many runs in which thousands of samples have been combusted [9,10]. X-ray diffraction was performed on a Rigaku Geiger Flex, 2-circle powder diffractometer at a generator tension of 50 kV and a current of 20 mA; scans were take from 2θ 1.5 to 10, step size 0.1 and scan time per step of 10 s. Bright field transmission electron microscopy (TEM) images of the composites were obtained at 60 kV with a Zeiss 10c electron microscope. The samples were ultramicrotomed with a diamond knife on Riechert-Jung Ultra-Cut E microtome at room temperature to give ∼70 nm thick sections. The sections were transferred from the knife-edge to 600 hexagonal mesh Cu grids. The contrast between the layered silicates and the polymer phase was sufficient for imaging, so no heavy metal staining of sections prior to imaging is required.

2.3. Preparation of 2-methyacryloyloxyethylhexadecyldimethylammonium bromide

The preparation of 2-methyacryloyloxyethylhexadecyldimethylammonium bromide was accomplished by a procedure which is similar to that in the literature [11]. A 31.4 g (0.200 mol) portion 2-(dimethyamino)ethylmethacrylate and 30.5 g (0.100 mol) 1-bromohexadecane were reacted at 50 °C in the presence of 3000 ppm of the inhibitor hydroquinone monomethyl ether in ethyl acetate for 24 h. After the mixture was cooled to room temperature, the white precipitant was filtered and washed with ethyl acetate, then it was dried in vacuum oven at room temperature for 24 h and 30.7 g product was produced (67% yield). ^{1}H NMR (300 MHz, D_2O, δ, ppm) δ 6.13 (s, 1H), 5.57 (s, 1H), 4.59 (broad, 2H), 3.80 (broad, 2H), 3.42 (broad, 2H), 3.21 (s, 6H), 1.85 (s, 3H), 1.67 (broad, 2H), 1.25 (s, 26H), 0.84 (m, 3H).

2.4. Preparation of methyl methacrylate oligomerically-modified clay with 12% clay loading (PMMA12 clay)

In a 500 mL 3-neck round bottom flask were placed 9.25 g (0.0200 mol) 2-methyacryloyloxyethylhexadecyldimethylammonium bromide (MHAB), 100 g (1.00 mol) of inhibitor-free methyl methacrylate (MMA), 11 g benzoyl peroxide (BPO) and 300 mL $CHCl_3$. The contents of the flask were stirred until all had dissolved at room temperature under a nitrogen flow, then it was refluxed for 4 h. After this time period, the mixture was quenched by the addition of methanol and the solvent was evaporated at low temperature and pressure. The resulting solid was dissolved in THF, then precipitated by the addition of methanol; 108 g of a white solid was recovered and the molecular weight was in the range of 3300 ± 1000, based on the Mark–Houwink constants for poly(methyl methacrylate).

A 16.6 g sample of the pristine sodium clay in 1000 mL distilled water and 500 mL THF was stirred at room temperature for 24 h. The oligomer prepared above, which was dissolved in 1200 mL of THF in a 2000 mL round bottom flask, was added drop-wise to the dispersed clay; a precipitate appeared immediately and the slurry was stirred at room temperature for 12 h. After the stirring was stopped, the supernatant liquid was poured off and a fresh mixture of H_2O/THF (40/60) was added and the slurry was stirred again for an additional 12 h at room temperature. The slurry was filtered and the precipitate was air-dried for 1 day and then in a vacuum oven at 40 °C for 48 h and the modified clay was obtained. The TGA curve of this clay gave a residue of 14% at 600 °C.

2.5. Preparation of methyl methacrylate oligomerically-modified clay with 22% clay loading (PMMA22 clay)

The same procedure as above was followed using 18.5 g (0.0400 mol) 2-methyacryloyloxyethylhexadecyldimethylammonium bromide, 100 g (1.00 mol) of inhibitor-free methyl methacrylate, 12.5 g benzoyl peroxide (BPO) and

Table 1
Composition of poly(methyl methacrylate) clay nanocomposites

Sample code	Inorganic clay in final product (%)	Modified clay amount (%)	Poly(methyl methacrylate) (%)
PMMA12 clay			
PMMA-12-01	1	8.3	91.7
PMMA-12-03	3	25.0	75.0
PMMA-12-05	5	42.0	58.0
PMMA22 clay			
PMMA-22-01	1	4.5	95.5
PMMA-22-03	3	13.6	86.4
PMMA-22-05	5	23.0	77.0
PMMA33 clay			
PMMA-33-01	1	3.0	97.0
PMMA-33-03	3	9.1	90.9
PMMA-33-05	5	15.0	85.0

300 mL $CHCl_3$. The TGA curve of this clay gave a residue of 24% at 600 °C.

2.6. Preparation of methyl methacrylate oligomerically-modified clay with 33% clay loading (PMMA33 clay)

The identical procedure as above was followed using 18.5 g (0.0400 mol) 2-methyacryloyloxyethylhexadecyldimethylammonium bromide, 50.06 g (0.0500 mol) of inhibitor-free methyl methacrylate, 6.9 g benzoyl peroxide (BPO) and 150 mL $CHCl_3$. The TGA curve of this clay gave a residue of 32% at 600 °C.

2.7. Preparation of polymer clay nanocomposites

All the nanocomposites prepared in this study were melt blended in a Brabender Plasticorder at high speed (60 rpm) at 230 °C for 15 min. The composition of each nanocomposite is calculated from the amount of clay and polymer charged to the Brabender, as shown in Table 1.

2.8. Measurement of molecular weight

The molecular weights were determined by intrinsic viscosity measurements using the relation $[\eta] = 7.0 \times 10^{-3} M_w^{0.71}$ in toluene at 30 °C [12]. The viscosity average molecular weight of the polymer was 3300 ± 1000.

3. Results and discussion

Previous studies have shown that a methacrylate copolymer modified clay (MAPS clay) did not show good compatibility with poly(methyl methacrylate) (PMMA) [13,14]. This surprising observation inspired this work, in which a new oligomerically-modified methacrylate-containing clay was produced by the reaction of dimethylaminoethyl methacrylate with methyl methacrylate. The reaction route for the formation of this oligomeric salt is shown in Fig. 1. According to the molecular weight (M_w = 3300) and reaction molar ratio, every 30 MMA units will contain 0.6 cation unit with PMMA12 clay; every 30 MMA units will contain 1.2 cation unit with PMMA22 clay, while every 30 MMA units will contain 2.4 cation unit with PMMA33 clay, thus the modified clays are expected to have one, two or at most three cations per chain.

3.1. X-ray diffraction (XRD) characterization of the nanocomposites

Figs. 2–4 present the XRD data for the PMMA clay and its nanocomposites. The *d*-spacing of MMT is about 1.2 nm and this increases to 3.5 nm with PMMA12 clay and PMMA22 clay and to 3.0 nm with PMMA33 clay. According to the ammonium salt per chain in the oligomer, the two or three cations in PMMA33 salt may result in either crowding in the gallery space or pinning of the clay layers, while the smaller number of cations in PMMA12 or PMMA22 salt may not

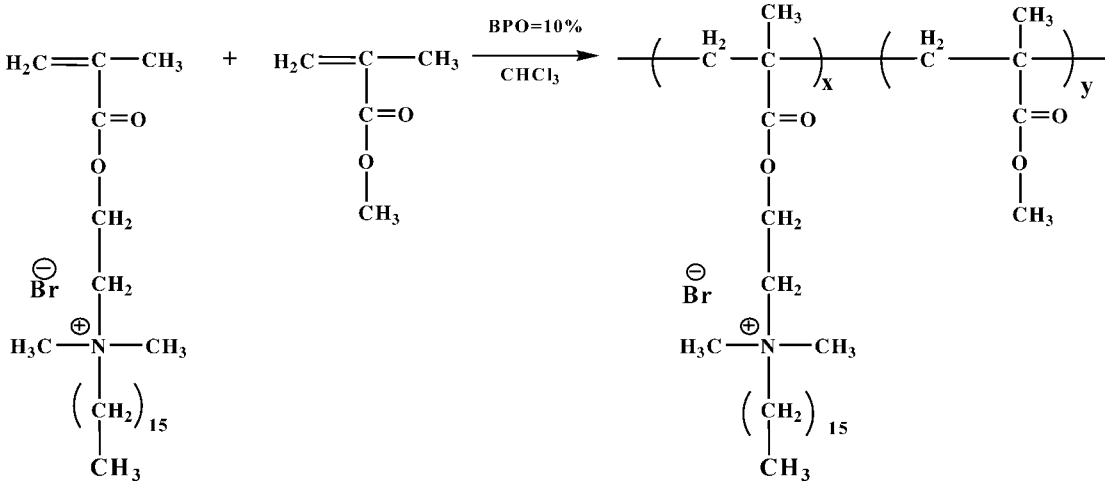

Fig. 1. The reaction route for the formation of the PMMA oligomer.

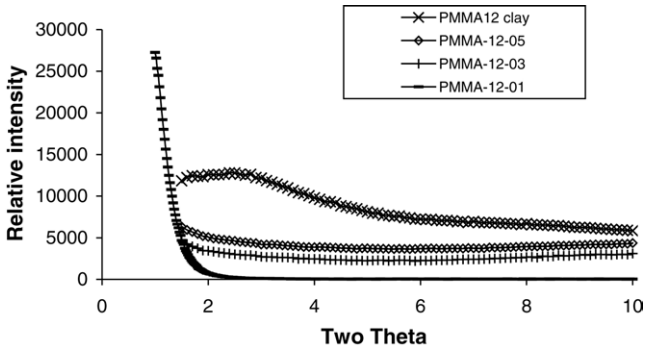

Fig. 2. XRD traces for PMMA12 clay and its PMMA nanocomposites. The numbers in the code refer to the amount of inorganic clay that is present.

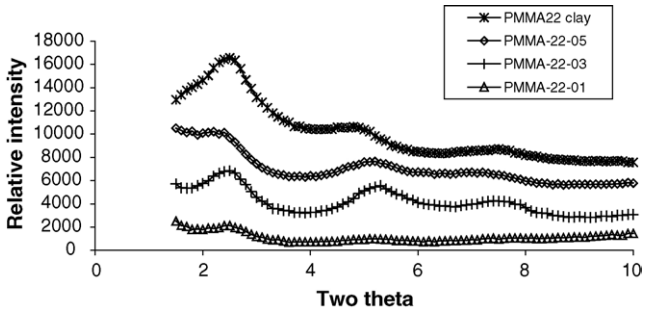

Fig. 3. XRD traces for PMMA22 clay and its PMMA nanocomposites. The numbers in the code refer to the amount of inorganic clay that is present.

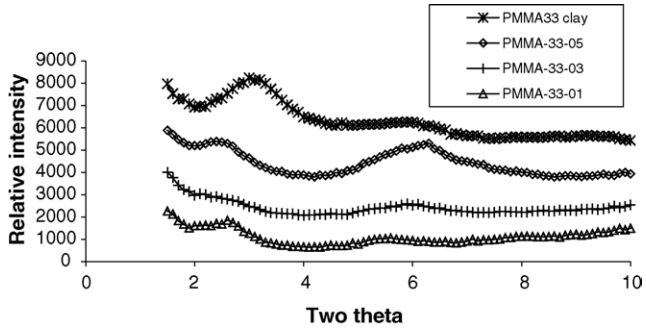

Fig. 4. XRD traces for PMMA33 clay and its PMMA nanocomposites. The numbers in the code refer to the amount of inorganic clay that is present.

be sufficient to cause pinning of the layers together. When these are clays melt blended with PMMA, no peaks can be seen with PMMA12 clay nanocomposite, which suggests the formation of either a delaminated system or a disordered system. The peaks are seen in the same position as in the clay for the PMMA22 clay nanocomposite, which suggests that either an intercalated structure has been formed or that no insertion has occurred and an immiscible system has been produced. The peaks shift to a lower 2θ for PMMA33 clay nanocomposite, indicating an increase in the *d*-spacing of these nanocomposites compared with modified clay, which could result from more insertion of polymer. Compared with PMMA22 clay nanocomposites, PMMA33 clay nanocomposites show broader peaks, which may indicate a greater tendency towards disordering for this material.

3.2. TEM characterization of nanocomposites

Transmission electron microscopy, TEM, is complementary to XRD, especially when peaks are not observed in XRD, since this technique provides an actual image of the clay. The low magnification image gives an idea of the nanodispersion while the high magnification image permits the identification of the morphology of the nanocomposite. Figs. 5–7 show the TEM images for the PMMA clay nanocomposites. At low magnification (left hand side), one can see that there is good nanodispersion of the clay in PMMA. At higher magnifications, one can see the individual clay layers for PMMA12 clay, while tactoids can be seen for PMMA22 clay. It is surprising that individual clay layers are clearly seen for the PMMA33 clay nanocomposites, some of which are in registry, indicating intercalation, while others have lost this registry, indicating delamination. All of these are best described as mixed intercalated/delaminated nanocomposites.

3.3. Thermagravimetric analysis (TGA) characterization of the nanocomposites

Table 2 and Figs. 8–10 provide TGA data and curves for the PMMA clay nanocomposites. The data includes the 10%

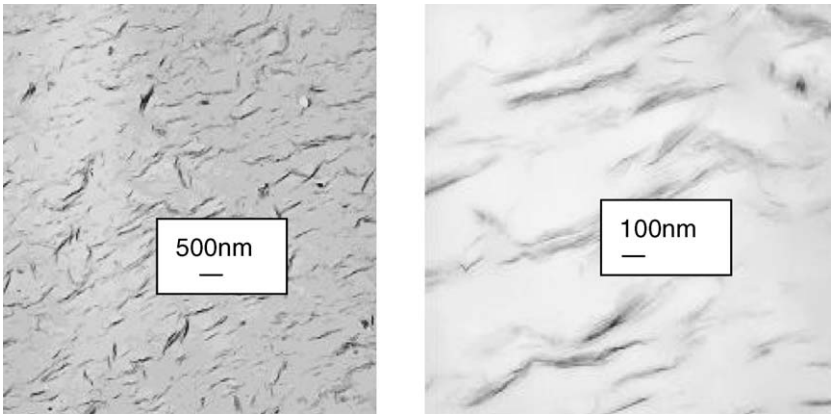

Fig. 5. TEM image at low (left) and high (right) magnification for PMMA melt blended with PMMA12 clay (3% inorganic clay).

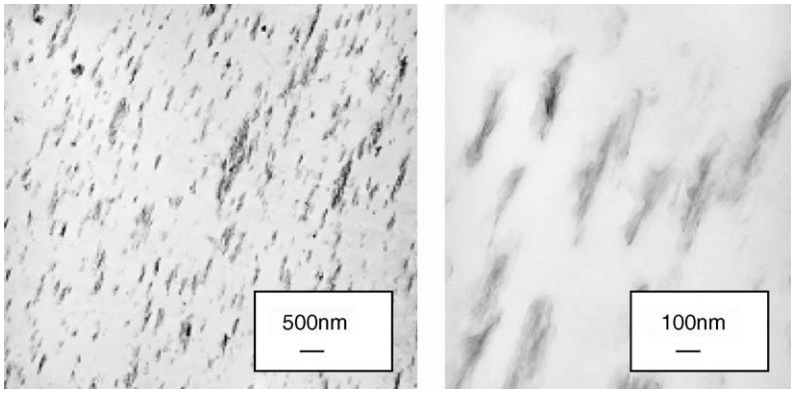

Fig. 6. TEM image at low (left) and high (right) magnification for PMMA melt blended with PMMA22 clay (3% inorganic clay).

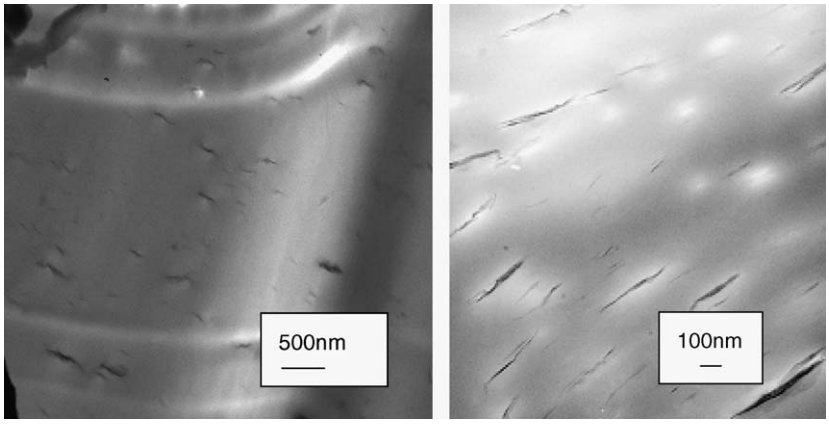

Fig. 7. TEM image at low (left) and high (right) magnification for PMMA melt blended with PMMA33 clay (3% inorganic clay).

degradation temperature, $T_{0.1}$, a measure of the onset temperature of the degradation, 50% degradation temperature, $T_{0.5}$, the mid-point of the degradation process, and the fraction of material which does not volatilize at 600 °C, denoted as char. Looking first of all at the clays before nanocomposite formation, one sees that the thermal stability of the clay, as evaluated by T_{10} and T_{50}, increases as the inorganic content of the clay increases. Since the inorganic clay has much better thermal stability than PMMA, this is to be expected. One can see from these data that all the nanocomposites exhibit an increase in the onset and mid-point temperature of degradation relative to virgin PMMA and it increases as the amount of the clay increases, which indicates that PMMA clay nanocomposites have enhanced thermal stability. This is a typical behavior for PMMA nanocomposites.

Table 2
TGA data of PMMA clay and its nanocomposites

	$T_{0.1}$ (°C)	$T_{0.5}$ (°C)	Char (%)
PMMA	271	339	0
PMMA12 clay	279	371	14
PMMA-12-01	318	383	1
PMMA-12-03	336	393	4
PMMA-12-05	338	401	6
PMMA22 clay	321	418	24
PMMA-22-01	308	377	2
PMMA-22-03	332	390	5
PMMA-22-05	337	398	8
PMMA33 clay	348	428	32
PMMA-33-01	310	377	2
PMMA-33-03	317	379	6
PMMA-33-05	351	397	8

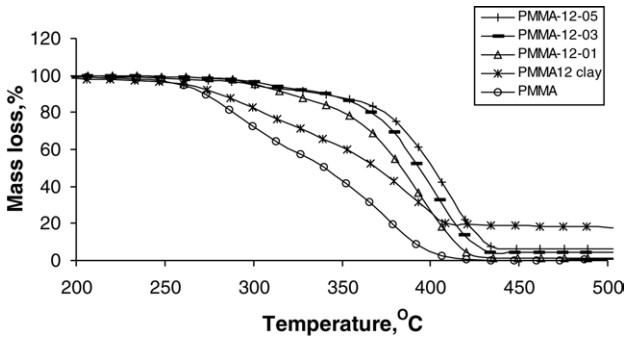

Fig. 8. TGA curve for PMMA12 clay and its PMMA nanocomposite.

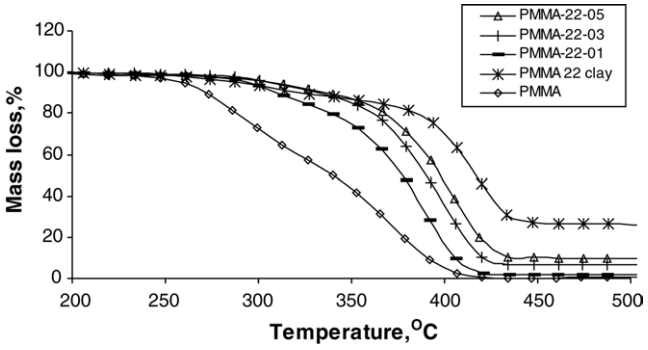

Fig. 9. TGA curve for PMMA22 clay and its PMMA nanocomposite.

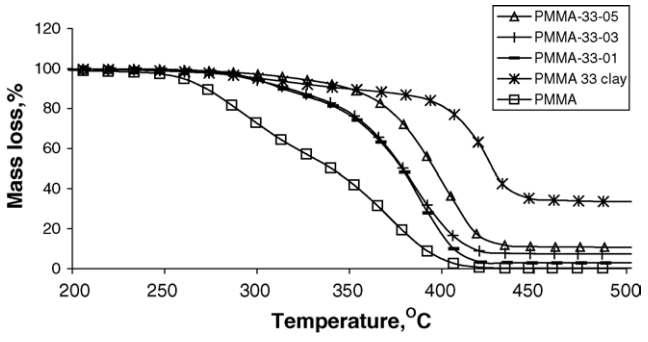

Fig. 10. TGA curve for PMMA33 clay and its PMMA nanocomposite.

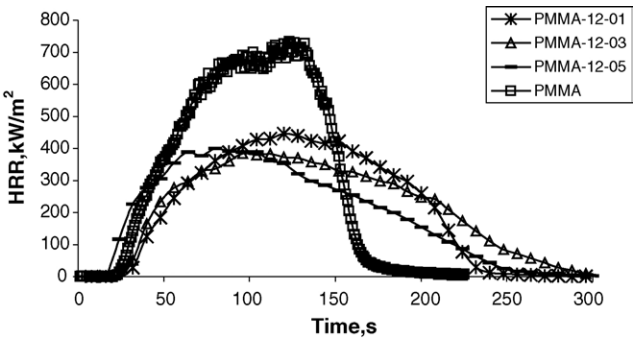

Fig. 11. Heat release rate curves for PMMA12 clay nanocomposites.

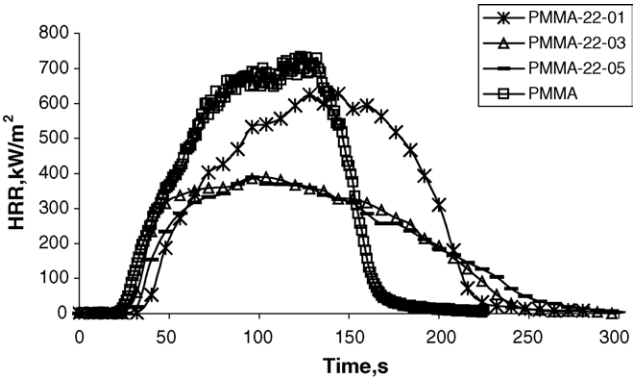

Fig. 12. Heat release rate curves for PMMA22 clay nanocomposites.

3.4. Cone calorimetric characterization of the nanocomposites

The fire properties of the nanocomposites were assessed by cone calorimetry and the results are shown in Table 3 and Figs. 11–13. The major parameters that may be obtained from the cone calorimeter include: the times to ignition and peak heat release rate; the heat release rate and especially its peak value, PHRR; the specific extinction area, SEA, a measure of smoke; and the mass loss rate, MLR, which normally tracks very well with changes in the peak heat release rate. From the data, one can see that the mass loss rate decreases, the time to ignition is increased and there is a substantial reduction in the peak heat release, in all cases, the PHRR reduction is around 45% with 3% inorganic clay, which is larger than has been previously observed for PMMA-clay nanocomposites [14]. This may be an indication that improved compatibility between PMMA and the modified clay has been obtained, leading to better nanodispersion. This large reduction in PHRR is in agreement with the XRD and TEM results which suggest that good nanodispersion has been obtained. The combination of XRD and TEM do not sample the bulk of the material and may, at times gives

Table 3
Cone calorimetry data for methyl methacrylate oligomerically-modified clay melt blended with poly(methyl methacrylate) at 35 kW/m²

Sample	Time to ignition (s)	PHRR[a] (kW/m²) (%reduction)[a]	Time to PHRR (s)	Total heat released (MJ/m²)	ASEA[a] (m²/kg)	MLR[a] (g/(s m²))
PMMA	25 ± 2	715 ± 21	128 ± 12	85 ± 5	168 ± 16	20 ± 1
PMMA-12-01	31 ± 2	466 ± 15 (35%)	114 ± 3	60 ± 2	236 ± 3	15 ± 1
PMMA-12-03	34 ± 2	425 ± 37 (41%)	111 ± 3	64 ± 1	251 ± 6	13 ± 1
PMMA-12-05	28 ± 4	440 ± 20 (38%)	114 ± 30	69 ± 4	261 ± 37	13 ± 1
PMMA-22-01	31 ± 5	645 ± 12 (10%)	126 ± 9	69 ± 5	173 ± 13	19 ± 0
PMMA-22-03	35 ± 3	377 ± 13 (47%)	100 ± 5	65 ± 4	243 ± 20	11 ± 1
PMMA-22-05	33 ± 2	368 ± 21 (49%)	104 ± 6	57 ± 0	290 ± 2	12 ± 1
PMMA-33-01	27 ± 1	478 ± 31 (33%)	152 ± 24	65 ± 2	207 ± 6	16 ± 1
PMMA-33-03	27 ± 0	394 ± 13 (45%)	88 ± 2	50 ± 5	274 ± 10	12 ± 1
PMMA-33-05	33 ± 1	372 ± 5 (48%)	81 ± 1	60 ± 1	216 ± 17	11 ± 1

[a] PHRR, peak heat release rate; % reduction = [PHRR (virgin polymer) − PHRR (nanocomposite)/PHRR (virgin polymer)]; ASEA, average specific extinction area; MLR: mass loss rate.

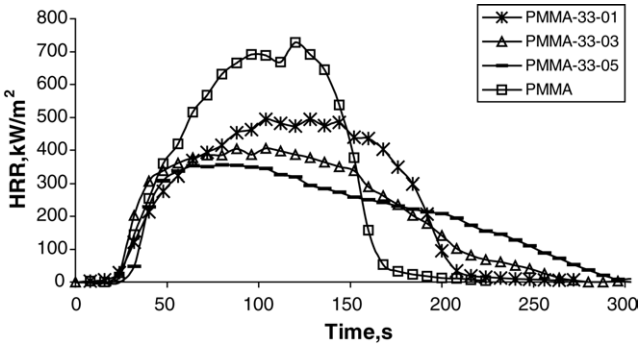

Fig. 13. Heat release rate curves for PMMA33 clay nanocomposites.

incorrect results because the area that is sampled may not be characteristic of the whole, but this is not true in this case.

4. Conclusions

The combination of 2-methyacryloyloxyethylhexadecyldimethylammonium bromide and methyl methacrylate produces a copolymer which can be used to obtain a modified clay which shows very good compatibility with methyl methacrylate. XRD and TEM reveal that the PMMA clay nanocomposite has good nanodispersion, which is in agreement with the results from cone calorimetry.

References

[1] M. Alexandre, P. Dubois, Mater. Sci. Eng. R28 (2000) 1–63.
[2] T.J. Pinnavaia, Science 220 (1983) 365–371.
[3] J. hu, C.A. Wilkie, Polym. Int. 49 (2000) 1158–1163.
[4] J. Zhu, F.M. Uhl, A.B. Morgan, C.A. Wilkie, Chem. Mater. 13 (2001) 4649–4654.
[5] J. Zhu, A.B. Morgan, F.J. Lamelas, C.A. Wilkie, Chem. Mater. 13 (2001) 3774–3780.
[6] S. Su, D.D. Jiang, C.A. Wilkie, Polym. Adv. Technol. 15 (2004) 225–231.
[7] C. Zeng, L.J. Lee, Macromolecules 34 (2001) 4098–4130.
[8] X. Huang, W. Brittain, Macromolecules 34 (2001) 3255–3260.
[9] J.W. Gilman, T. Kashiwagi, M. Nyden, J.E.T. Brown, C.L. Jackson, S. Lomakin, E.P. Giannelis, E. Manias, in: S. Al-Malaika, A. Golovoy, C.A. Wilkie (Eds.), Chemistry and Technology of Polymer Additives, Blackwell Scientific, 1999, pp. 249–265.
[10] J.W. Gilman, T. Kashiwagi, E.P. Giannelis, E. Manias, S. Lomakin, J.D. Lichtenham, P. Jones, in: M. Le Bras, G. Camino, S. Bourbigot, R. Delobel (Eds.), Fire Retardancy of Polymeric Materials, The Use of Intumescence, Royal Society of Chemistry, Cambridge, 1998, pp. 203–221.
[11] W. Zhang, Y. Liang, W. Luo, Y. Fang, J. Polym. Sci. Part A; Polym. Chem. 41 (2003) 3218–3226.
[12] J. Brandrup, E.H. Immergut, E.A. Grulke (Eds.), Polymer Handbook, fourth ed., John Wiley & Sons, New York, 1999, p. VII/16.
[13] S. Su, D.D. Jiang, C.A. Wilkie, Polym. Degrad. Stab. 83 (2004) 333–346.
[14] S. Su, D.D. Jiang, C.A. Wilkie, Polym. Degrad. Stab. 83 (2004) 321–331.